J. Environ. Nanotechnol.
Volume 3, No.4 (2014) pp. 67-72
ISSN (Print): 2279-0748
ISSN (Online): 2319-5541
doi: 10.13074/jent.2014.12.144111

Titania Nanoparticles Modified with Nitrogen: Enhanced Visible-light Photocatalytic Activity

Gurulakshmi Mariappan[1], Periyasami Vijayan[2], Chinnathambi Suresh[3], Kannan Shanthi[4]*

[1]*Department of Chemistry, Madras Christian College (Autonomous), Tambaram, Chennai, TN, India.*
[2]*Department of Chemistry, Chikkanna Govt. Arts College, Tirupur, TN, India.*
[3]*Electrodics and electrocatalysis Division, CSIR-Central Electro Chemical Research Institute, Karaikudi, TN, India*
[4*]*Department of Chemistry, Anna University, Chennai, TN, India.*

Received:07.09.2014 Accepted:05.12.2014

Abstract

Titanium dioxide (TiO_2), for instance, is one of the most popular and promising materials in heterogeneous photocatalytic application. Several attempts have been made to induce bathochromic (red) shifts of the band gap of Titania in order to utilize the solar light. In this study we have reportedthe synthesis of nitrogen doped TiO_2 nanoparticles by sol-gel method using urea and ammonia as the nitrogen source and by direct oxidation of TiN were tested for visible-light photocatalytic degradation of methylene blue and phenol. The catalysts were characterized by N_2 adsorption desorption studies, X-ray diffraction and Diffuse reflectance UV-visible spectroscopy techniques. The chemically modified TiO_2 shows strong absorption for visible light and high activities for the degradation of methylene blue and phenol aqueous solution. The presence of two different surface states characteristics of Pure and nitrogen doped TiO_2 was confirmed by the shift in absorption from 398 nm to 405 nm and 409 nm from the DRUV-Visible spectral results. The spherical morphology of the catalysts was observed from the SEM images.

Keywords: *Ammonia; Nitrogen modification; Photocatalytic activity; Titanium Nitride; Urea; Visible-light.*

1. INTRODUCTION

Rapid Industrialisation cause great environmental problems due to generation and buildup of toxic wastes. The widespread disposal of wastewater from textile and food industries containing organic dyes into land and water bodies has led to serious contamination in many countries worldwide. About 1–20% of the total global production of dyes is lost during the dyeing process and is released into the environment as textile effluent (Houas *et al.* 2001; Rafols and Barcelo, 1997; Weber and Stickney, 1993). Many dyes are highly water-soluble in order to meet the color requirement of deep dyeing. Some dyes even possess toxicity that is hazardous to aquatic life. Those effluents which contain high amounts of dyes; decreases water transparency, hinder sunlight penetration, thus disturbing photosynthetic activity and also gas solubility, damaging the environment (Guaratini and Zanoni, 2000). The discharge of such effluents also undergoes chemical and biological changes that cause excessive oxygen demand in the receiving water and then a treatment is required before discharge into ecosystems (Davydov *et al.* 2001).

Traditional methods for treating the textile effluent consist of various chemical, physical, and biological processes. For example, Liu *et al.* (2002) investigated the treatment of direct dye wastewater by coagulation; Sanghi and Bhattacharya (2002) studied the adsorption–coagulation for the decolorisation of textile dye solutions; Beydilli *et al.* (2000) reported the possibility of decolorization of azo dye biologically; Liakou *et al.* (2003) studied a combined chemical and biological treatment of wastewater containing azo dyes. Koyuncu (2003) studied the treatment and reuse of both synthetic and industrial dyes by nanofiltration membranes. Consequently, weathering of organic dyes through these traditional treatment methods are increasingly ineffective due to high cost and also produce toxic metabolites, which impart adverse effects on animal and human health

* **Kannan Shanthi** Tel.no: +919840146642
E-mail: kshanthiramesh@yahoo.com

(Forgas *et al*. 2004). The increased public concern has promoted the need to develop novel treatment methods.

As one of the novel advanced oxidation process, the heterogeneous photocatalytic oxidation process developed in the 1970s is of special interest especially when solar light is used. Amongst various oxide semiconductor photocatalysts, titanium dioxide has proven to be the most popular and promising material. In addition, for TiO_2 the threshold or ideal wavelength corresponding to the band-gap energy of 3.21 eV is at near ultraviolet radiation ($\lambda > 400$ nm). Further, TiO_2 absorbs only 5 % energy of the solar spectrum; hence research is focused in developing TiO_2 materials which can utilize more amount of solar energy (Fujishima and Honda, 1972; Fox and Dulay, 1993). Several attempts have been made to induce bathochromic (red) shifts of the band gap of Titania. One of the initial approaches was the doping of TiO_2 with transition-metal elements such as Co, Ag, Pt, W or V to form $Ti_{1-x}A_xO_2$ compounds (Choi *et al.* 1994). Another approach showed that narrowing the desired band gap of TiO_2 could be achieved by replacing lattice oxygen with anionic dopant species, such as F, N, C or S to produce oxygen deficient titania ($TiO_{2-x}X_{2x/n}$) (Asahi *et al.* 2001; Bahneman, 2000; Ohno *et al.* 2003; Liu *et al.* 2009 and Ren *et al.* 2007).

In this study, we have reported the discoloring of aqueous solutions of methylene blue (MB), commonly used in textile industry and phenol, commonly found in industrial effluent, in a slurry photocatalytic reactor in the presence of suspended nitrogen doped TiO_2 nanoparticles, prepared by sol-gel method (using Urea or ammonia) and also by direct oxidation method (using TiN). The prepared powders were characterized by XRD, DRUV-Vis, and BET techniques. The efficiency of the N-TiO_2 was studied for the degradation of MB and phenol, and, the results are discussed with reference to the physico-chemical properties.

2. EXPERIMENTAL

Titanium tetraisopropoxide (Alfa Aesar, 95 %), Titanium nitride (Sigma Aldrich, 99 %), Absolute ethanol (Hayman Limited, 99.9 %), Thiourea (SRL, 99.9 %) and MB (Plazo Laboratories Pvt. Ltd.,) were used without further purification. De-ionised water was used throughout this study. The pH of the solution was adjusted by using 0.1 N HCl or NaOH solutions.

2.1 Catalyst Preparation

Nitrogen doped TiO_2 was prepared by two different methods viz. sol-gel and direct oxidation method. The first set of Nitrogen doped *TiO_2* was prepared by sol-gel method as follows: Titanium tetraisopropoxide (TTIP) was dissolved in 20 ml of ethanol and hydrolysed using 50 ml of H_2O:Ethanol (1:1) mixture to give white precipitate. Urea (U) was dissolved in 20 ml of H_2O and added dropwise to the above solution with constant vigorous stirring. The resulting mixture was stirred well for 2 h and kept for ageing (6 h) at room temperature. The precipitate was then filtered and dried in an oven at 330 K. Thus obtained white colour powder was calcined at 773 K for 3 h to obtain yellow coloursulphur-doped TiO_2. The TTIP:U molar ratio corresponds to 1:2 and 1:4 were denoted as $NTiO_2$(U2) and $NTiO_2$(U4), respectively.

The second set of Nitrogen doped *TiO_2* was prepared by direct oxidation of titanium nitride at different temperature (673, 773, 873, and 973 K). The catalysts prepared were denoted as $NTiO_2$(673), $NTiO_2$(773), $NTiO_2$(873) and $NTiO_2$(973). For comparison the nitrogen doped TiO_2 was also prepared by sol-gel method using ammonia as the nitrogen precursor and denoted as $NTiO_2(NH_3)$. The synthesis of the un-doped TiO_2 follows the same procedure in the absence of urea and denoted as TiO_2.

2.2. Catalyst Characterization

The synthesized samples were characterized by powder *X-ray diffraction (XRD)* spectrometer with Phillips X'pert model using Cu-Kα radiation. XRD patterns were recorded from 20º - 70º (2θ) by step scanning with a step size of 0.02º θ. The average crystallite size (<D>) of the synthesized catalysts was calculated by applying the Scherrer's equation (Kim *et al.* 2008):

$$<D> = k \lambda / \beta \cos \theta \qquad (1)$$

where k (0.94) is the Scherrer constant, λ is the X-ray wavelength (0.1548 nm), β the full-width at half-maximum of crystal plane (101) and θ is the diffraction angle of the crystal plane (101).

UV-Visible diffuse reflectance spectra of the powders were recorded using Shimadzu UV2450 model with $BaSO_4$ as the reference.

N_2adsosrption desorption isotherms were measured at 77 K on a Belsorp mini, BEL Japan system. Prior to analysis the samples were pretreated at 473 K for 2 h under nitrogen atmosphere.

The *SEM images* were recorded using ESEM Quanta 200 FEI Scanning Electron Microscopy.

2.3 Photocatalytic reactor set-up

The visible-light photocatalytic efficiency of the nitrogen modified TiO_2 nanoparticles was measured for the degradation of MB and phenol in an aqueous solution. Photocatalytic degradation was performed in a home-made slurry batch visible-light photoreactor. The details of the photoreactor have been discussed in our previous report (Gurulakshmi *et al*. 2012). 100 mL of 20 ppm reactant solution was taken in a glass tube and oxygen was bubbled into the solution throughout the experiment. An aliquot of 10 mL of sample was collected at particular time interval and the catalyst was separated by centrifugation. The filtered samples were then analyzed by UV-Visible spectrophotometer and TOC analyzer. The kinetics of photocatalytic reactions can be described as pseudo first order where C_0 and C_t are MB concentrations initially and after time "*t*", respectively and the rate constants (k, min^{-1}) determined from plots of ln (C_0/C_t) versus irradiation time (Kim *et al.* 2008).

3. RESULTS & DISCUSSION

3.1 X-ray Diffraction

The crystal structure of the synthesized catalysts was analysed by powder X-ray diffraction technique.

Fig. 1 shows the XRD patterns of TiO_2 and $NTiO_2$ prepared by sol-gel and direct oxidation method. XRD patterns of nitrogen doped TiO_2 synthesizedby sol-gel method using urea and ammonia as the nitrogen source ($NTiO_2$(U2); $NTiO_2$(U4) and $NTiO_2(NH_3)$) shows the characteristic peaks corresponding to anatase TiO_2 with different crystal planes, the peak corresponding to (101) plane diffraction located at 2θ=25.4° (JCPDS 21-1272) (Saha and Tompkins, 1992; Sathish *et al.* 2005).

The decrease in the average crystallite size as evident from Table 1; may be due to the suppressed crystallite growth in the TiO_2 lattice as the nitrogen ions replaces O^{2-} ions from the lattice. XRD pattern also reveals that the doping of nitrogen by sol-gel method does not favor the phase transformation of anatase to rutile or brookite form. However, the nitrogen doped TiO_2 prepared by direct oxidation of TiN results in the formation anatase type TiO_2 with slight shift in 2θ values at 773 K and further transforms to rutile at higher temperature above 873 K. The amount of nitrogen dopant present in each catalyst is estimated from the CHN analysis is listed in Table 1.

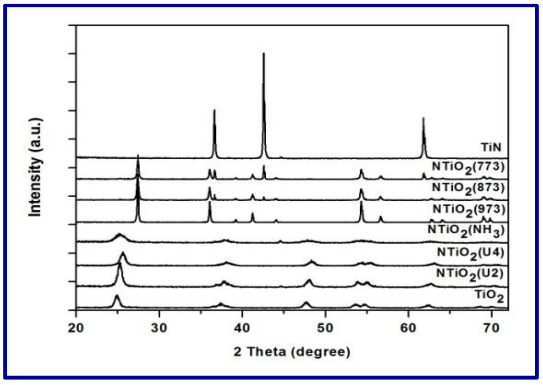

Fig. 1: XRD patterns of TiO_2, TiN and various $NTiO_2$ prepared by sol-gel and direct oxidation method

3.2. Diffuse Reflectance UV-visible Spectra

The UV-Visible diffuse reflectance spectra of TiO_2 and $NTiO_2$ prepared by sol-gel and direct oxidation methods are shown in Figure 2. Compared to the spectrum of pure titania (TiO_2), a shift to the lower energy region and a new absorption shoulder were clearly observed for the nitrogen modified titania.

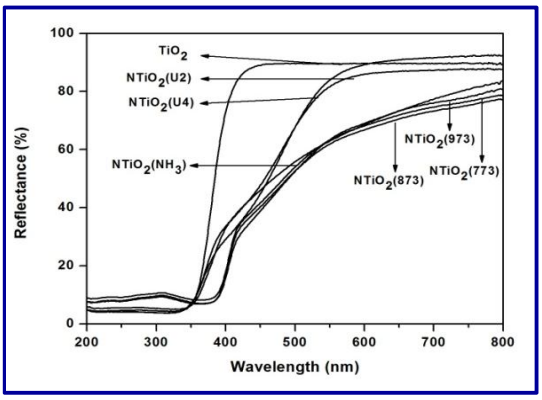

Fig. 2: DRUV-visible spectra of TiO_2 and various $NTiO_2$ prepared by sol-gel and direct oxidation method

The noticeable observed shift of absorbance shoulder from 399 nm to the visible-light region (450-550 nm) are due to the p-states of N atom contributing to band gap narrowing by mixing with O 2p states. Further more, the absorbance of N-doped TiO_2 shows two band transitions at 399 nm, accounted for the TiO_2 fundamental band transitions and around 450-550 nm, as a resultant of N doping (18,19).

Table 1. Physico-chemical characteristics and photocatalytic activity of various catalysts

Catalyst	[a] Crystallite Size (nm)	[b] Band gap energy (eV)	[c] S_{BET} (m^2/g)	[d] Nitrogen Content	[e] *Rate constant (k)* x 10^{-3} min^{-1}	[e] R^2 Value
TiO_2	31.6	3.11	81.6	-	3.94	0.9892
$NTiO_2$(U2)	27.97	3.02 and 2.25	45.3	0.28	7.18	0.9945
$NTiO_2$(U4)	24.63	3.01 and 2.21	74.9	0.37	7.98	0.9961
$NTiO_2$(773)	ND	2.95 and 2.10	27.9	7.01	5.33	0.9932
$NTiO_2$(873)	ND	2.96 and 2.12	24.6	1.92	5.91	0.9940
$NTiO_2$(973)	ND	2.94 and 2.11	16.3	0.31	4.77	0.9894
$NTiO_2(NH_3)$	16.32	2.96 and 2.10	90.3	0.41	8.73	0.9969

a – Calculated using the Scherrer equation (Equation :1) b – Calculated using Eg = 1240/λ

c – Calculated from BET d – Estimated from the CHN Analysis

e – Rate constant, *k* is calculated from the linear fitting on ln (C0/Ct) versus reaction time for MB degradation. ND – Not determined

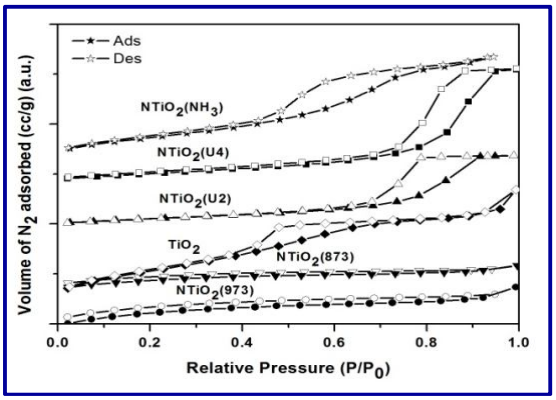

Fig. 3: N_2 adsorption-desorption isotherm TiO_2; $NTiO_2$(U4); $NTiO_2$(U2); $NTiO_2(NH_3)$; $NTiO_2$(873)and $NTiO_2$(973)

The corresponding band gap energies estimated from the absorption edges (Table 1) are determined by the equation: Eg = 1239.8 / λ, where Eg is the band-gap energy (eV) and λ is the wavelength of the absorption edges (nm) in the spectrum. These results also show that the nitrogen atoms are incorporated into the lattice of TiO_2, thus altering its crystal and electronic structures.

Nitrogen adsorption desorption isotherms obtained for TiO_2 and nitrogen doped TiO_2 prepared by sol-gel and direct oxidation methods are shown in Figure 3. Type IV isotherm with type H2 hysteresis was observed for $NTiO_2$(U4); $NTiO_2$(U2) and $NTiO_2(NH_3)$ catalysts, confirming mesoporosity. It is also observed that no mesoporosity was found in $NTiO_2$(773) and $NTiO_2$(873) obtained by direct oxidation of TiN. BET analysis results are cited in Table 1. $NTiO_2(NH_3)$ obtained by sol-gel method using ammonia as nitrogen source shows high surface area (90.3 m^2/g). The morphology of the following catalysts: TiO_2, $NTiO_2$(U4), $NTiO_2(NH_3)$ and $NTiO_2$(873) were presented in Figure 4. The morphology was found to be spherical in shape. The nitrogen modification does not alter the morphology of the catalysts. The morphology of $NTiO_2$(873) catalyst synthesized by direct oxidation method shows some flake-like morphology along with spherical morphology.

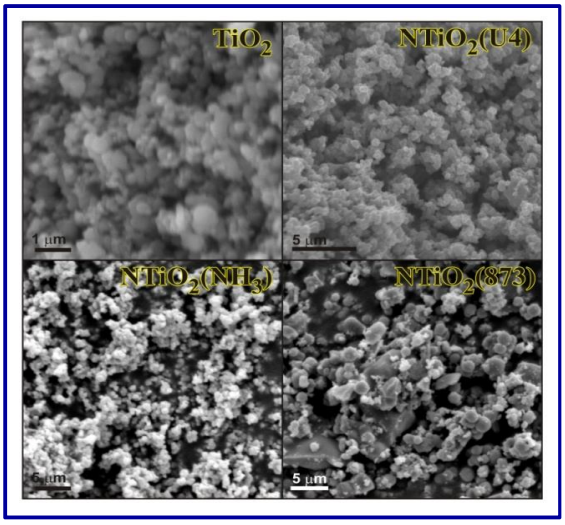

Fig. 4: SEM images of TiO_2, $NTiO_2$(U4), $NTiO_2(NH_3)$ and $NTiO_2$(873) prepared by sol-gel and direct oxidation method

From Figure 5 it is found that all the reactions follow pseudo-first-order kinetics. The degradation of MB under visible light irradiation catalyzed by nitrogen modified TiO_2 prepared by different method was compared with pure TiO_2. The apparent rate constant, *k* is calculated from the linear

fitting on ln (C_0/C_t) versus reaction time and is listed in Table 1. The $NTiO_2(NH_3)$ obtained by sol-gel method using ammonia as nitrogen source containing anatase phase with high surface area exhibit high photocatalytic activity (k=8.73 x 10^{-3} min^{-1}) under the present experimental conditions. The complete degradation of MB was attained at 5 h in all the catalysts.

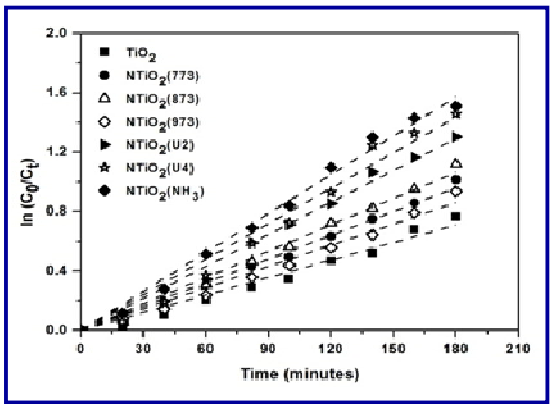

Fig. 5: Photocatalytic Degradation of MB under visible light irradiation

Reaction Conditions : MB Concentration – 30 ppm; Visible-light source – Tungsten Halogen lamp (λ> 410 nm); pH – 3.5; In the presence of Oxygen flow. Product Analysis – UV-visible spectrophotometer**.**

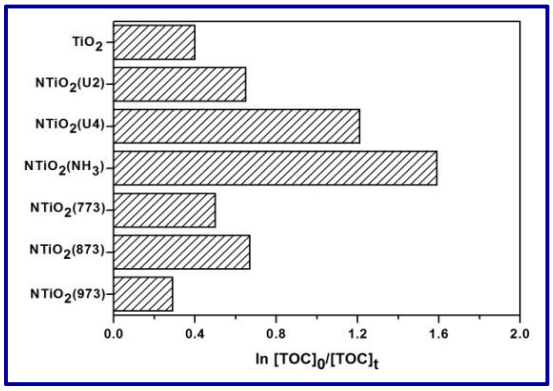

Fig. 6: Effect of nitrogen doping on photocatalytic degradation of Phenol under visible light irradiation

Reaction Conditions : Phenol Concentration – 30 ppm; Visible-light source – Tungsten Halogen lamp (λ> 410 nm); pH – 3.5; In the presence of Oxygen flow; Time – 6h; Product Analysis – Total Organic Carbon Analyzer**.**

The visible-light photocatalytic degradation of phenol by pure TiO_2 and nitrogen modified TiO_2 by different method at 6h of reaction is shown in Figure 6. The same trend in activity was observed for phenol degradation on all the catalysts as in MB degradation. However, complete degradation of phenol was achieved only after 8 h of reaction time under the same experimental conditions.

4. CONCLUSION

Nitrogen doped TiO_2 nanoparticles were synthesized by sol-gel method using urea and ammonia as the nitrogen source and by direct oxidation of TiN. The visible-light absorption capacity of the nitrogen modified TiO_2 is evident from the diffuse reflectance spectra. The presence of two different surface states characteristics of Pure and nitrogen doped TiO_2 was confirmed by the shift in absorption from 398 nm to 405 nm and 409 nm from DRUV-Visible spectral results. The order of activity found is as follows: $NTiO_2(NH_3)$ > $NTiO_2(U4)$ > $NTiO_2(U2)$ ≈ $NTiO_2(873)$ > $NTiO_2(773)$ > $NTiO_2(973)$. From this study it is concluded that the method of doping of nitrogen greatly influences the visible-light Photocatalytic activity.

ACKNOWLEDGEMENT

The authors are thankful to DRDO, UGC-DRS and DST-FIST for providing instrumentation facility at the Department of Chemistry, Anna University, Chennai, India.

REFERENCES

Asahi, R., Morikawa, T., Ohwaki, T., Aoki, K., Taga, Y., Visible-light photocatalysis in nitrogen-doped titanium oxides, *Science*., 293, 269–271(2001). doi:10.1126/science.1061051

Bahnemann, D. W., Current challenges in photocatalysis: Improved photocatalysts and appropriate photoreactor engineering, *Res. Chem. Intermed.*, 26, 207-220(2000). doi:10.1163/156856700X00255

Beydilli, M. I., Pavlostathis, S. G. and Tincher, W. C., Biological decolorization of the azo dye Reactive Red 2 under various oxidation-reduction conditions, *Water Environ. Res.,* 72, 698-705(2000). doi:10.2175/106143000X138319

Rafols, C. and Barcelo, D., Determination of mono- and disulphonatedazo dyes by liquid chromatography–atmospheric pressure ionization mass spectrometry, *J. Chromatogr. A.,* 777, 177–192(1997). doi:10.1016/S0021-9673(97)00429-9

Choi, W., Termin, A. and Hoffmann, M. R., The role of metal ion dopants in quantum-sized TiO_2: correlation between photoreactivity and charge carrier recombination dynamics, *J. Phys. Chem.,* 98, 13669-13679 (1994). doi:10.1021/j100102a038

Davydov, L., Reddy, E. P., France, P., and Smirniotis P. G., Sonophotocatalytic destruction of organic contaminants in aqueous systems on TiO_2 powders, *Appl. Catal. B.,* 32, 95–105(2001). doi:10.1016/S0926-3373(01)00126-6

Forgas, E., Cserhati, T. and Oros, G., Removal of synthetic dyes from wastewater: A review, *Environ. Intl*., 30, 953–971(2004). doi:10.1016/j.envint.2004.02.001

Fox, M. A. and Dulay, M. T., Heterogeneous Photocatalysis, *Chem. Rev*., 93, 341-357(1993). doi:10.1021/cr00017a016

Fujishima, A. and Honda, K., Electrochemical photolysis of water at a semiconductor electrode, *Nature,* 238, 37-3 (1972). doi:10.1038/238037a0

Guaratini, C. and Zanoni, M., Textile Dyes, Quimica Nova. 23, 71–79(2000). doi:10.1590/S0100-40422000000100013

Gurulakshmi, M., Selvaraj, M., Selvamani, A., Vijayan, P., SasiRekha, N. R., and Shanthi, K., Enhanced visible-light photocatalytic activity of V_2O_5/S–TiO_2 nanocomposites, *Appl. Catal*. A:Gen., 449, 31–46(2012). doi:10.1016/j.apcata.2012.09.039

Houas, A., Lachheb, H., Ksibi, M., Elaloui, E., Guillard, C. and Herrmann. J. M., Photocatalytic degradation pathway of methylene blue in water, *Appl. Catal. B*., 31, 145–157(2001). doi:10.1016/S0926-3373(00)00276-9

Kim, S. W., Khan, R., Kim, T. J., and Kim, W. J., Visible-light induced Photocatalytic degradation of 4–chlorophenol and phenolic compounds in aqueous suspension of pure Titania: Demonstrating the existence of a surface-complex mediated path, *Bull. Korean Chem. Soc.* 29, 6-9(2008).

Koyuncu, I., Direct filtration of Procion dye bath wastewaters by nanofiltration membranes: flux and removal characteristics, *J. Chem. Tech. Biotechnol*., 78, 1219-1224(2003). doi:10.1002/jctb.924

Liakou, S., Zissi, U., Kornaros, M. and Lyberatos, G., Combined chemical and biological treatment of azo dye-containing wastewaters, *Chem. Eng. Commun*., 190, 645-661(2003). doi:10.1080/00986440302108

Liu, J., Qin, W., Zuo, S., Yu, Y. and Hao, Z., Solvothermal induced phase transition and visible photocatalytic activity of nitrogen-doped titania, *J. Hazard. Mater*., 163, 273-278(2009). doi:10.1016/j.jhazmat.2008.06.086

Liu, R. L. H., Chiu, H. M. and Yeh R. Y. L., Colloid interaction and coagulation of dye wastewater with extra application of magnetites, *Int. J. Environ. Stud.,* 59, 143-158(2002). doi:10.1080/00207230211965

Ohno, T., Mitsui, T. and Matsumura, M., Photocatalytic activity of S-doped TiO2 photocatalyst under visible light, *Chem. Lett.,* 32 364-365(2003). doi:10.1246/cl.2003.364

Ren, W., Ai, Z., Jia, F., Zhang, L., Fan, X. and Zou, Z., Low temperature preparation and visible light photocatalytic activity of mesoporous carbon-doped crystalline TiO2, *Appl. Catal., B: Environ*., 69, 138-144(2007). doi:10.1016/j.apcatb.2006.06.015

Saha, N. C. and Tompkins, H. G., Titanium nitride oxidation chemistry: An X-ray photoelectron spectroscopy study, *J. Appl. Phys*., 72, 3072-3080(1992). doi:10.1063/1.351465

Sanghi, R. and Bhattacharya, B., Review on decolorisation of aqueous dye solutions by low cost adsorbents, *Res. J. Can*.,118, 256-269(2002).

Sathish, M., Viswanathan, B., Viswanath, R. P. and Gopinath, C. S., DFT studies on hetero atom (N or/and S) substitution in TiO2*, Chem. Mater.,* 17, 6349-6353(2005). doi:10.1021/cm052047v

Weber, E. J. and Stickney, V. C., Hydrolysis kinetics of Reactive Blue 19-Vinyl Sulfone, *Water Res.,* 27, 63–67(1993). doi:10.1016/0043-1354(93)90195-N